Chinese Chemical Letters 37 (2026) 111478

Contents lists available at ScienceDirect

Chinese Chemical Letters

journal homepage: www.elsevier.com/locate/cclet

Immobilization of multiple hydrogen-bond acceptor sites in a stable cage-based framework for efficient C_2F_6 purification

Yongqin Zhu[a,b,1], Zhenyu Ji[a,b,1], Yunzhe Zhou[a,c], Mingyan Wu[a,c,*]

[a] State Key Lab of Structural Chemistry, Fujian Institute of Research on the Structure of Matter, Chinese Academy of Sciences, Fuzhou 350002, China
[b] College of Chemistry, Fuzhou University, Fuzhou 350108, China
[c] University of Chinese Academy of Sciences, Beijing 100049, China

ARTICLE INFO

Article history:
Received 21 May 2025
Revised 12 June 2025
Accepted 17 June 2025
Available online 18 June 2025

Keywords:
Electronic specialty gases
Cage-based framework
C_2F_6 purification
Gas separation
Metal-organic framework

ABSTRACT

The efficient removal of CF_3CH_2F and CF_3CHF_2 to obtain high-purity C_2F_6 is of critical importance for electronics industry but remains a big challenge. Currently, few adsorbents have been developed for one-step purification of C_2F_6 from multicomponent perfluorocarbons and hydrofluorocarbons mixtures. Herein, we report a metal-organic framework (FJI-W20) with multiple immobilized hydrogen-bond acceptors including F, O, N atoms which can form hydrogen bonds interactions with the H atoms of CF_3CH_2F and CF_3CHF_2, prompting it high selectivities for CF_3CH_2F/C_2F_6 and CF_3CHF_2/C_2F_6. More importantly, the special cage-like structure in turn ensures the high adsorption capacities of CF_3CH_2F and CF_3CHF_2. Adsorption experiments show that FJI-W20 can absorb 132.9 cm^3/g of CF_3CH_2F and 110.1 cm^3/g of CF_3CHF_2 but only adsorb 57.9 cm^3/g of C_2F_6 at 298 K and 1 bar, delivering the selectivities as high as 17.6 and 12.3 for CF_3CH_2F/C_2F_6 (5/95, v/v) and CF_3CHF_2/C_2F_6 (5/95, v/v). Practical breakthrough experiments indicate that FJI-W20 can purify C_2F_6 from $CF_3CH_2F/CF_3CHF_2/C_2F_6$ (5/5/90, v/v/v) in one step at different gas flow rates as well as various temperatures and 20.6 mol/kg of high-purity (≥99.99 %) C_2F_6 can be directly obtained under ambient conditions.

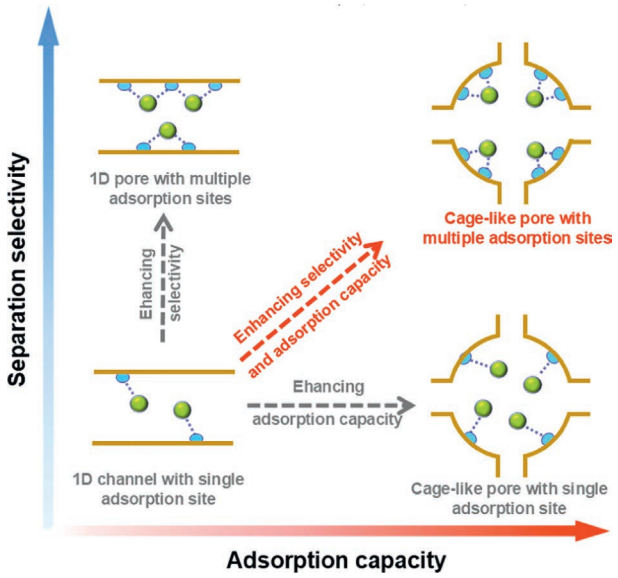
© 2026 Published by Elsevier B.V. on behalf of Chinese Chemical Society and Institute of Materia Medica, Chinese Academy of Medical Sciences.

Electronic specialty gases (ESGs), especially fluorinated gases (F-gases), play pivotal roles in the advancement of semiconductor and microelectronics industries [1–7]. Hexafluoroethane (C_2F_6) as an important perfluorinated electronic specialty is highly preferred in the advanced electronics industry for its excellent etching performance, high chemical stability, low global warming potential (GWP), and low production cost [8–10]. In industry, C_2F_6 is predominantly manufactured by fluorinating 1,1,1,2-tetrafluoroethane (CF_3CH_2F) and pentafluoroethane (CF_3CHF_2), so that small amounts of CF_3CH_2F or CF_3CHF_2 would invariably remain in the crude product [11]. Given the extremely similar boiling points (CF_3CH_2F, 246.7 K; CF_3CHF_2, 224.6 K; C_2F_6, 195.1 K) and electronic-grade purity requirement, it is difficult and energy-consuming to obtain high purity C_2F_6 industrially using cryogenic distillation methods [12–15].

Adsorptive separation process has been increasingly regarded as the most promising gas purification technology due to its high efficiency and low energy consumption [16–18]. With the flourishing of adsorbents in the past decade, numerous tricky separations alkanes/alkenes [19–22], alkynes/alkenes [23–26], aromatics/cyclic aliphatics [27–30] and so on have been achieved. However, in contrast to the above gas mixtures, the carbon atoms in C_2F_6, CF_3CH_2F and CF_3CHF_2 are all sp^3 hybridized, with fluorine atoms being the main component of molecules [31–34]. This means that the physico-chemical properties of the three gases are much closer. Presently, no clear separation mechanism has been developed for the separation of C_2F_6 from $CF_3CH_2F/CF_3CHF_2/C_2F_6$ mixture. Compared to C_2F_6, both CF_3CH_2F and CF_3CHF_2 have hydrogen atoms in their molecules. Owing to the electron-withdrawing effect of the F atom, the C–H bonds in CF_3CH_2F and CF_3CHF_2 are highly polarized and the H atoms are relatively active [35–37]. As a result, the H atoms in CF_3CH_2F and CF_3CHF_2 are good hydrogen-bond donors. As such, constructing adsorbents with high degree of hydrogen-bond acceptor sites should allow for selective adsorption of CF_3CH_2F and CF_3CHF_2 [38–41]. Firmly, in the previous reports, J. Milner, Motkuri and Su *et al.* have proven that halogen (X), O or N atoms in the frameworks can form X/O/N···H hydrogen bonds with the hydrogen atoms of hydrofluorocarbons to enhance their adsorption [42–44]. Thus, if we functionalize multiple hydrogen bond acceptors in the framework, the selectivities for CF_3CH_2F and CF_3CHF_2 can be similarly improved.

* Corresponding author.
E-mail address: wumy@fjirsm.ac.cn (M. Wu).
[1] These authors contributed equally to this work.

https://doi.org/10.1016/j.cclet.2025.111478
1001-8417/© 2026 Published by Elsevier B.V. on behalf of Chinese Chemical Society and Institute of Materia Medica, Chinese Academy of Medical Sciences.



Scheme 1. The strategy of immobilizing multiple hydrogen-bond acceptors as the adsorption sites in a cage-like framework to consturct the efficient CF_3CH_2F/CF_3CHF_2-selective adsorbent.

As we know, an eligible adsorbent should not only have good gas selectivity, but also a high adsorption capacity, so as to achieve efficient separation performance [45–48]. However, adsorbents with narrow channels often possess high gas selectivity but often show low adsorption capacity because of the strict pore size limitations or immobilization of functional sites will drastically reduce their porosity. It is widely known that cage-like materials have high gas uptakes due to their extremely large cavities which can accommodate many gas molecules [49–53]. Consequently, if we can construct a porous material with both cage-like cavities and multiple hydrogen-bond acceptors, high CF_3CH_2F and CF_3CHF_2 adsorption capacity and high CF_3CH_2F/C_2F_6, CF_3CHF_2/C_2F_6 selectivity could be achieved simultaneously (Scheme 1).

With the above consideration in mind, we herein report a cage-like metal–organic framework FJI-W20. On its pore surface, multiple hydrogen-bond acceptors such as F, O and N atoms that can provide tight C–H···F, C–H···O and C–H···N interactions with CF_3CH_2F and CF_3CHF_2 molecules are modified. As expected, FJI-W20 exhibits simultaneous preferential and high adsorption for CF_3CH_2F and CF_3CHF_2. Adsorption experiments show that it can absorb 132.9 cm^3/g of CF_3CH_2F and 110.1 cm^3/g of CF_3CHF_2 but can only absorb 57.9 cm^3/g of C_2F_6 at 298 K and 1 bar. Due to the large difference in their uptakes, FJI-W20 delivers selectivity as high as 17.6 and 12.3 for respective CF_3CH_2F/C_2F_6 (5/95, v/v) and CF_3CHF_2/C_2F_6 (5/95, v/v). Breakthrough experiments show that high-purity C_2F_6 can not only be obtained from the binary CF_3CH_2F/C_2F_6 (5/95, v/v) and CF_3CHF_2/C_2F_6 (5/95, v/v) mixtures but also can be directly collected from ternary $CF_3CH_2F/CF_3CHF_2/C_2F_6$ (5/5/90, v/v/v) mixture. After one breakthrough experiment at 298 K and 1 bar, the productivity of C_2F_6 can reach 20.6 mol/kg. Furthermore, FJI-W20 can maintain its good separation performance at different gas flow rates and temperatures. Computational simulation reveals that multiple electronegative atoms on the pore wall of FJI-W20 can generate substantial hydrogen bonding interactions with CF_3CH_2F and CF_3CHF_2, which facilitates the FJI-W20 to achieve an eye-catching $CF_3CH_2F/CF_3CHF_2/C_2F_6$ separation performance.

FJI-W20 can be afforded as dark orange block-shaped crystals by solvothermal method (Fig. S1 in Supporting information). Single-crystal X-ray experiments reveal that it crystallizes in the $I4_1/amd$ space group (Table S1 in Supporting information). As depicted in Fig. 1a, FJI-W20 is constructed by three components, *i.e.*, BDC–CF_3^{2-} anion, BIPYDZ ligand and $[Co_8(\mu_3\text{-}OH)_4(H_2O)_4(SO_4)_2(COO)_8]$ cluster (Co_8 cluster). In the Co_8 cluster unit of, Co_1 atom is six-coordinated by two carboxylate oxygen atoms from two BDC–CF_3^{2-} ligands, two oxygen atoms of two μ_3-OH groups, one oxygen atom from SO_4^{2-}, one water oxygen atom and one nitrogen atom from BIPYDZ, leading to octahedral geometry [54]. Analogously, the coordination mode of Co_2 atom in this Co_8 cluster is also hexa-coordination, which is completed by two carboxylate oxygen atoms from two BDC–CF_3^{2-} ligands, two oxygen atoms of μ_3-OH groups and two oxygen atoms of SO_4^{2-} anion, respectively. In the structure of FJI-W20, each Co_8 cluster can bind to twelve linker ligands (eight BDC–CF_3^{2-} ligands and four BIPYDZ) (Fig. 1e). This unusual Co_8-based cluster node, in conjunction with two linear ligands BDC–CF_3^{2-} and BIPYDZ, jointly constructs a 3D framework with a unique cage-like structure (Fig. 1b). The solvent accessible volume in fully evacuated FJI-W20 is up to 59.2 % [55]. In FJI-W20, there are two kinds of polyhedral cages, that is, small tetrahedral cage (Cage-A) which is completed by three Co_8 clusters, four BDC–CF_3^{2-} ligands and one BIPYDZ ligand and big octahedral cage (Cage-B) which is completed by eight Co_8 clusters, eight BDC–CF_3^{2-} ligands and four BIPYDZ ligands (Figs. 1c and d). Especially, in simultaneous cage-A and cage-B, there are multiple electronegative atoms distributed, such as the F atoms, N atoms and O atoms, which are potential strong hydrogen bond receptors. This indicates that FJI-W20 can provide strong interactions with the gas molecules with the partially positive hydrogen atoms, such as CF_3CH_2F and CF_3CHF_2, thereby increasing the selectivity of CF_3CH_2F/C_2F_6 and CF_3CHF_2/C_2F_6.

The PXRD patterns of the as-synthesized FJI-W20 sample are well consistent with the calculated ones from the single crystal, indicating that the prepared FJI-W20 sample has high phase purity (Fig. S2 in Supporting information). Furthermore, FJI-W20 possesses excellent stability in air and common organic solvents, which can be certificated by the well matched PXRD patterns with the fresh sample after imposing FJI-W20 in air for 30 days or various organic solvents for 7 days (Figs. S2 and S4 in Supporting information). What is more, FJI-W20 also demonstrates good thermal stability. The thermogravimetric analysis experiment (TGA) shows that there is no obvious weight loss up to 290 °C (Fig. S3 in Supporting information). Variable-temperature PXRD (VT-PXRD) were also carried out and the results show that no significant changes in the PXRD patterns are observed even at 200 °C in air atmosphere, implying that the framework can be maintained at such high temperature (Fig. S5 in Supporting information). On the whole, the excellent structural stability endows it with great Given the exceptional stability and large pore of FJI-W20, we next tested its gas adsorption properties. The 77 K N_2 was firstly employed to illustrate its porosity. As revealed in Fig. S6 (Supporting information), it can absorb 419.9 cm^3/g of N_2 at 77 K and 1 bar. The calculated BET surface area is up to 1640.4 m^2/g and the pore volume is as high as 0.65 cm^3/g, which indicates that FJI-W20 can be used as a promising platform for gas adsorption. Furthermore, owing to the cage-like structure and multiple hydrogen bond acceptors on its pore surface, it can be reasonably inferred that FJI-W20 may exhibits great potential for absorbing gas molecules that possess active hydrogen atoms.

Based on this inference, we immediately afterwards carried out the adsorption experiments for CF_3CH_2F, CF_3CHF_2 and C_2F_6. As anticipated, FJI-W20 showcases simultaneous high uptakes for CF_3CH_2F and CF_3CHF_2 in the wide temperature range. As shown in Figs. 2a–c, at 273 K and 100 kPa, the adsorption amounts for CF_3CH_2F and CF_3CHF_2 are up to 150.0 and 128.0 cm^3/g, respectively. When elevating the temperature to 298 K, the saturated uptakes of CF_3CH_2F and CF_3CHF_2 are 132.9 and 110.1 cm^3/g. And

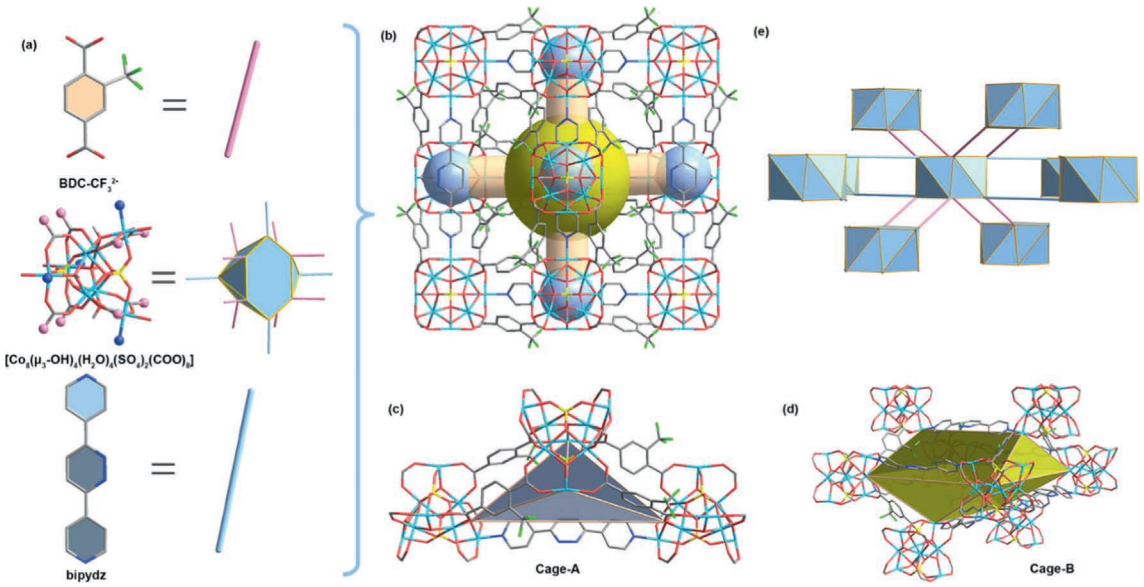


Fig. 1. Single-crystal X-ray structure of FJI-W20. (a) The subunits of FJI-W20. (b) Cage-like structure of FJI-W20. Solvent molecules and hydrogen atoms are omitted for clarity. (c) The structure of tetrahedron cage-A. (d) The structure of octahedron cage-B. (e) The 12-connected Co_8 cluster.

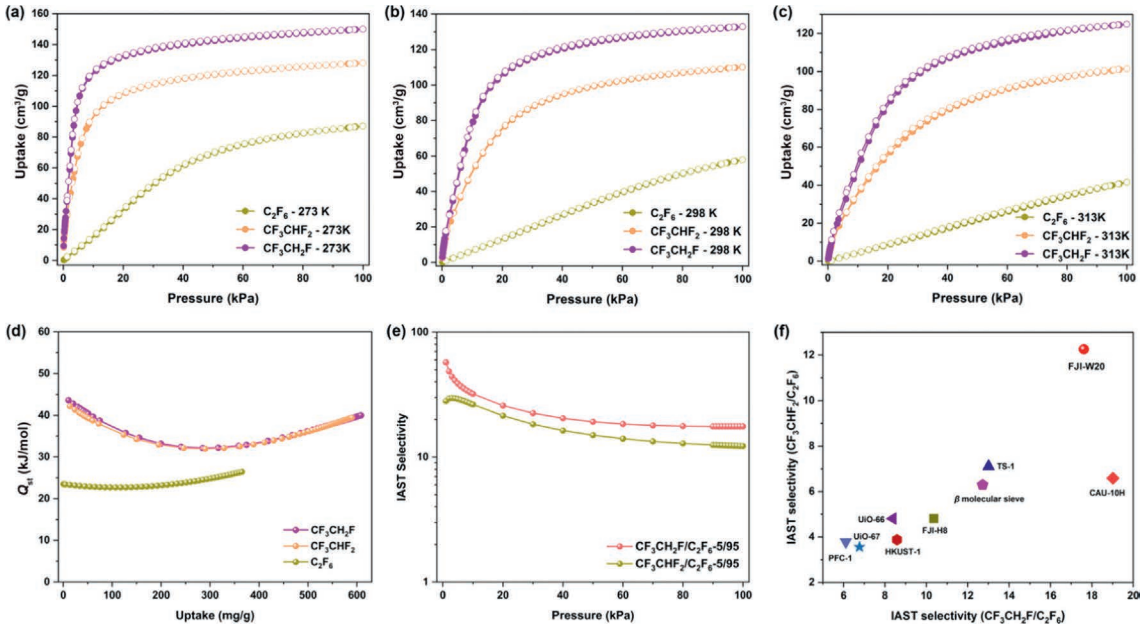


Fig. 2. Single-component adsorption isotherms of CF_3CH_2F, CF_3CHF_2 and C_2F_6 at (a) 273 K, (b) 298 K and (c) 313 K. (d) The Q_{st} for CF_3CH_2F, CF_3CHF_2 and C_2F_6 respectively. (e) IAST selectivity of FJI-W20 for CF_3CH_2F/C_2F_6 (5/95) and CF_3CHF_2/C_2F_6 (5/95). (f) Comparison of CF_3CH_2F/C_2F_6 (5/95) and CF_3CHF_2/C_2F_6 (5/95) selectivity of FJI-W20 and other materials.

the adsorption capacity remained almost perfectly consistent in the five consecutive adsorption cycles (Figs. S7–S9 in Supporting information). Notably, even the temperature is increased to 313 K, FJI-W20 can still absorb 124.9 cm^3/g of CF_3CH_2F and 101.5 cm^3/g of CF_3CHF_2. These results demonstrate that the cage based structure of FJI-W20 promotes its gas absorption capacity, which is unmatched by narrow pore materials such as $Ni(pba)_2$ that we previously reported [11]. Furthermore, comparing with the high storage capacity of CF_3CH_2F and CF_3CHF_2, FJI-W20 shows relatively low uptake for C_2F_6. The saturated uptakes of C_2F_6 by FJI-W20 at 273, 298 and 313 K are only 87.1, 57.9 and 41.6 cm^3/g, which is much lower than that of CF_3CHF_2 and CF_3CH_2F. More importantly, at low pressure region, the adsorption curves of C_2F_6 increase particularly gently, reflecting that the framework can hardly generate strong interaction with C_2F_6 [56–58]. Evidently, the adsorption results reveal that FJI-W20 shows great difference between fluoroethane such as CF_3CH_2F, CF_3CHF_2 and C_2F_6. And the apparently strong affinity for CF_3CH_2F and CF_3CHF_2 relative to C_2F_6 suggests that multiple hydrogen bond receptors in FJI-W20 may favour binding of hydrofluorocarbons.

In order to visually illustrate that FJI-W20 exhibits stronger interactions on CF_3CH_2F, CF_3CHF_2 than C_2F_6, we calculated the adsorption heats (Q_{st}) for CF_3CH_2F, CF_3CHF_2 and C_2F_6 with the adsorption isotherms at 273 and 298 K. As demonstrated in Fig. 2d and Figs. S13-S15 (Supporting information), the Q_{st} values at zero loading for CF_3CH_2F, CF_3CHF_2 are 43.6 and 42.2 kJ/mol, respectively. In contrast, the corresponding Q_{st} for C_2F_6 is 23.5 kJ/mol, indicating its lower affinity relative to CF_3CH_2F, CF_3CHF_2. This

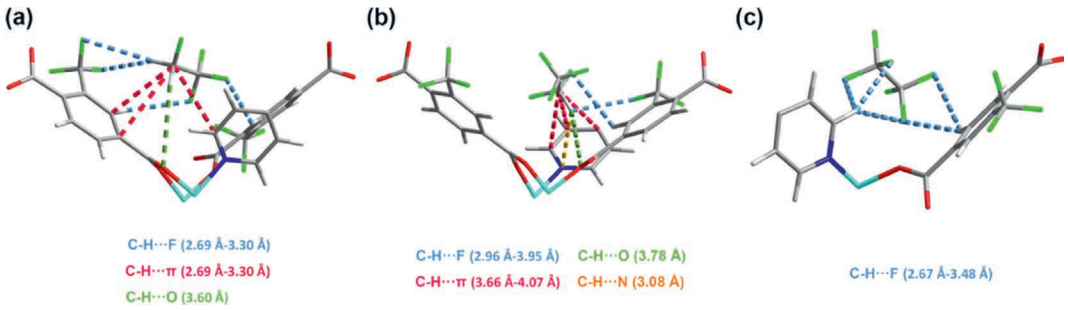


Fig. 3. The calculated preferential adsorption sites for (a) CF_3CH_2F, (b) CF_3CHF_2 and (c) C_2F_6 in FJI-W20. The C–H···F, C–H···O and C–H···N hydrogen bonds are respectively shown in dashed blue, dashed green and dashed orange lines. The C–H···π interactions between gas molecule and the pore surface are shown in dashed red lines.

difference may be attributed to the presence of electronegative atoms in the structure of FJI-W20, which enhances the framework-hydrofluorocarbon interactions. Given the remarkable affinity for CF_3CH_2F and CF_3CHF_2, we judge that it has the ability to purify C_2F_6 from $CF_3CH_2F/CF_3CHF_2/C_2F_6$ mixture. To validate this inference, ideal adsorbed solution theory (IAST) has been employed to determine the IAST selectivity (Figs. S10–S12 in Supporting information). As shown in Figs. 2e and f, the IAST selectivities for CF_3CH_2F/C_2F_6 (5/95) and CF_3CHF_2/C_2F_6 (5/95) can reach 17.6 and 12.3 at 298 K and 1 bar, which are much higher than other porous materials such as some commercial molecular sieves (12.7/6.3 for β molecular sieve and 13.0/7.1 for TS-1) and the cage-like porous materials without recognized sites (8.6/3.9 for HKUST-1, 8.4/4.8 for UiO-66 and 10.4/4.8 for FJI-H8) (Figs. S16–S37 and Table S2 in Supporting information). And this result sufficiently proves that FJI-W20 can be used as an efficient adsorbent to separate CF_3CH_2F/C_2F_6 and CF_3CHF_2/C_2F_6 and completely indicates that the immobilization of multiple hydrogen-bond acceptor sites in a cage-like metal-organic framework is a verifiable strategy for efficient C_2F_6 purification.

In order to further study the mechanism of FJI-W20 preferentially adsorbing CF_3CH_2F and CF_3CHF_2, theoretical calculations were carried out. As we know, compared with C_2F_6, CF_3CH_2F and CF_3CHF_2 contain not only F atoms, but also partially positive H atoms. The presence of H atoms enables CF_3CH_2F and CF_3CHF_2 to have more interactions with the skeleton. Therefore, the Q_{st} values of CF_3CH_2F and CF_3CHF_2 in FJI-W20 are higher than C_2F_6. According to Figs. 3a and b, the calculated results clearly reveal that CF_3CH_2F and CF_3CHF_2 molecules are tightly bound in the corners of the polyhedral hole that possessing abundant F/O/N environment. Specifically shown in Fig. 3a, CF_3CH_2F possesses eight interactions with FJI-W20, including four C–H···F hydrogen bonds ($D_{H\cdots F}$ = 2.69, 2.83, 3.27 and 3.30 Å), three C–H···π interactions ($D_{C\cdots C}$ = 3.58, 3.89 and 3.98 Å) and one C–H···O interactions ($D_{H\cdots O}$ = 3.60 Å) [59–63]. As depicted in Fig. 3b, each CF_3CHF_2 molecule interacts with the framework through two C–H···F ($D_{H\cdots F}$ = 2.96 and 3.95 Å), one C–H···N ($D_{H\cdots N}$ = 3.08 Å), one C–H···O ($D_{H\cdots O}$ = 3.78 Å) and three C–H···π ($D_{C\cdots C}$ = 3.66, 3.76 and 4.07 Å) supramolecular interactions. These evidences validate that the electronegative sites on the pores are critical for capturing CF_3CH_2F and CF_3CHF_2 molecules [64–67]. As a sharp contrast, there are complete F atoms in C_2F_6 molecule and it can only interact with the framework by C–H···F hydrogen bonds ($D_{H\cdots F}$ = 2.67, 2.79, 2.82, 3.42 and 3.48 Å) (Fig. 3c). Correspondingly, the calculated static binding energies of CF_3CH_2F, CF_3CH_2F and C_2F_6 are 52.12, 47.71 and 32.09 kJ/mol, respectively, which is in well agreement with the experimental trend of Q_{st} under zero coverage. These simulation results demonstrate the rationality of FJI-W20 as a purified C_2F_6 adsorbent.

Based on the above compelling rationales, we next conducted dynamic breakthrough experiments to investigate the practical performance of FJI-W20 for the purification of C_2F_6. Firstly, the binary gas mixture of CF_3CH_2F/C_2F_6 and CF_3CHF_2/C_2F_6 were employed to evaluate the C_2F_6 purification potentiality. As shown in Figs. 4a and b, FJI-W20 can effectively purify C_2F_6 from CF_3CH_2F/C_2F_6 and CF_3CHF_2/C_2F_6 respectively. In Fig. 4a, it can be seen that the C_2F_6 effluxes rapidly at 30.9 min whereas the signal of CF_3CH_2F emerges after 391.2 min. High-purity C_2F_6 (≥99.99 %) can be collected continuously during 360.3 min with an ultrahigh yield of 35.7 mol/kg. Similarly, FJI-W20 can also achieve efficient CF_3CHF_2/C_2F_6 separation (Fig. 4b). At 298 K and with the flow rate of 2.2 mL/min, high purity of C_2F_6 can be ceaselessly obtained from 30.9 min to 297.8 min and the corresponding C_2F_6 yield is as high as 25.9 mol/kg. The purification yield of C_2F_6 from CF_3CHF_2/C_2F_6 is slightly lower than from the CF_3CH_2F/C_2F_6 and this is owing to the lower adsorption capacity of FJI-W20 for CF_3CHF_2.

Motivated by the confirmed separation performance of binary mixtures for FJI-W20, we further assessed the C_2F_6 purification capacity from ternary C_2F_6-containing gas mixture of $CF_3CH_2F/CF_3CHF_2/C_2F_6$. As demonstrated in Fig. 4c, FJI-W20 can likewise realize high-efficiency separation of C_2F_6 from $CF_3CH_2F/CF_3CHF_2/C_2F_6$ in the breakthrough experiments, in which C_2F_6 first breaks the packed column, while CF_3CHF_2 and CF_3CH_2F are retained in adsorbent for a period of time. From the breakthrough curve, it can be seen that the sequence of gas outflow at the outlet is C_2F_6, CF_3CHF_2 and CF_3CH_2F, the result is coincident with the gas adsorption amounts. After one three-component separation experiment, about 20.6 mol/kg of high-purity C_2F_6 can be collected. Furthermore, six consecutive breakthrough experiments on FJI-W20 show that the breakthrough times and productivities of C_2F_6 express no obvious loss (Fig. 4d), indicating that FJI-W20 possesses excellent reusability in C_2F_6 purification process. Moreover, in consideration of the practical industrial situations, the adsorbent should keep good separation performance at different gas flow rates and high temperatures. Thus, in order to examine the separation capacity of FJI-W20 in near-actual conditions, we conducted the breakthrough experiments under different flow rates and high temperatures. As shown in Figs. 4e and f, FJI-W20 could maintain good C_2F_6 purification ability within the flow rates of 1.7–3.8 mL/min and the C_2F_6 productivities can even remain roughly unchanged, which implies that the separation performance of FJI-W20 could not be influenced by the flow rates. More than that, FJI-W20 as well works well under high temperatures. As depicted in Fig. 4g, when we gradually elevated the testing temperature, the separation time of C_2F_6 only shows slightly decrease. For instance, the temperature is increased to 318 K, the separation time of C_2F_6 is *ca.* 182.1 min and the corresponding C_2F_6 productivity is *ca.* 13.8 mol/kg (Fig. 4h). Remarkably, after exposure to air for 7 days, the separation performance is almost the same as that of fresh samples, which is rarely seen in previous reports (Fig. 4i). On the whole, above results suggest that FJI-W20 can realize good separation performance under the actual situations.

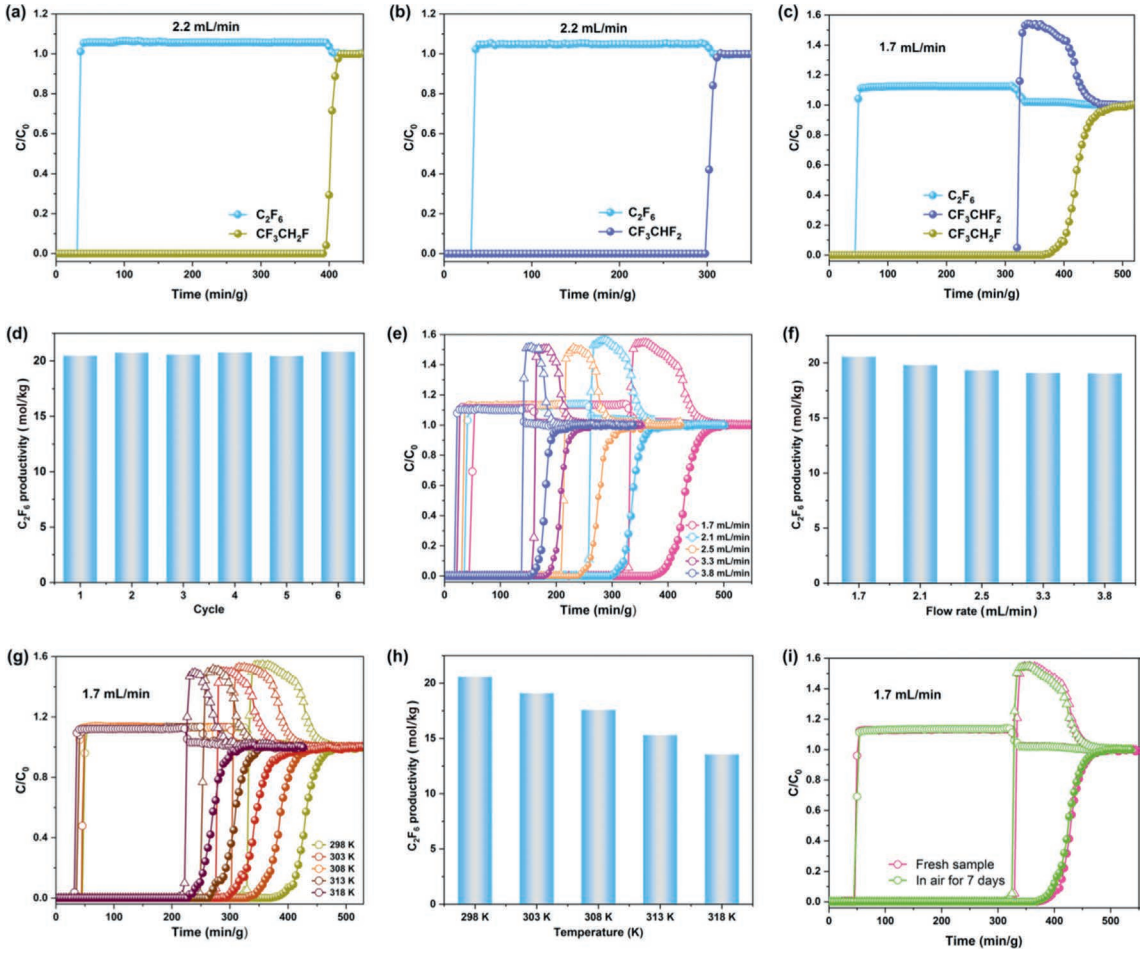


Fig. 4. The breakthrough experiments of (a) CF_3CH_2F/C_2F_6 (5/95, v/v), (b) CF_3CHF_2/C_2F_6 (5/95, v/v) and (c) $CF_3CH_2F/CF_3CHF_2/C_2F_6$ (5/5/90, v/v/v) at 298 K. (d) Six-cycle C_2F_6 yields for $CF_3CH_2F/CF_3CHF_2/C_2F_6$ (5/5/90, v/v/v) at 298 K with gas flow rate of 1.7 mL/min. (e) The breakthrough experiments of $CF_3CH_2F/CF_3CHF_2/C_2F_6$ (5/5/90, v/v/v) with the different flow rates. (f) C_2F_6 productivity for $CF_3CH_2F/CF_3CHF_2/C_2F_6$ (5/5/90, v/v/v) under different flow rates. (g) The breakthrough experiments of $CF_3CH_2F/CF_3CHF_2/C_2F_6$ (5/5/90, v/v/v) at differrent temperatures. (h) C_2F_6 productivity for $CF_3CH_2F/CF_3CHF_2/C_2F_6$ (5/5/90, v/v/v) at different temperatures. (i) Breakthrough experiment for $CF_3CH_2F/CF_3CHF_2/C_2F_6$ (5/5/90, v/v/v) after exposure to air for 7 days.

In summary, herein we report a cage-based framework FJI-W20 whose pore surface is functionalized with multiple electronegative F, O and N atoms as hydrogen-bond acceptors. Cage-like pores and multiple hydrogen-bond sites between the framework and hydrofluoroethanes ensure selectively capture of CF_3CH_2F and CF_3CHF_2 with high uptakes. For example, at 298 K and 1 bar, FJI-W20 can absorb 132.9 cm^3/g of CF_3CH_2F and 110.1 cm^3/g of CF_3CHF_2 but only 57.9 cm^3/g of C_2F_6. The selectivity of CF_3CH_2F/C_2F_6 (5/95, v/v) and CF_3CH_2F/C_2F_6 (5/95, v/v) can reach 17.6 and 12.3. Separation experiments indicate that FJI-W20 can purify C_2F_6 with high purity from ternary $CF_3CH_2F/CF_3CHF_2/C_2F_6$ mixtures. After one separation cycle, 20.6 mol/kg of high-purity C_2F_6 can be directly obtained from $CF_3CH_2F/CF_3CHF_2/C_2F_6$ (5/5/90, v/v/v) mixture. Additionally, at different gas flow rates and temperatures high-purity C_2F_6 can also be obtained in one step. This work illustrates that our strategy of immobilizing multiple hydrogen-bond acceptor sites in a cage-like framework is highly successful and effective for designing novel porous materials of purifying of C_2F_6 from CF_3CH_2F and CF_3CHF_2.

CRediT authorship contribution statement

Yongqin Zhu: Writing – original draft, Software, Investigation, Formal analysis, Data curation. **Zhenyu Ji:** Writing – original draft, Conceptualization. **Yunzhe Zhou:** Project administration, Formal analysis. **Mingyan Wu:** Writing – review & editing, Funding acquisition.

Declaration of competing interest

The authors declare that they have no known competing financial interests or personal relationships that could have appeared to influence the work reported in this paper.

Acknowledgments

This work is supported by the National Natural Science Foundation of China (NSFC, No. 22271282) and the Strategic Priority Research Program of the Chinese Academy of Sciences (No. XDB1170000). This work is also supported by the Self-deployment Project Research Program of Haixi Institutes, Chinese Academy of Sciences (No. CXZX-2022-JQ04) as well as Fujian Science & Technology Innovation Laboratory for Optoelectronic Information of China (No. 2021ZR120).

Supplementary materials

Supplementary material associated with this article can be found, in the online version, at doi:10.1016/j.cclet.2025.111478.

References

[1] A.J. Sicard, R.T. Baker, Chem. Rev. 120 (2020) 9164–9303.
[2] Z. Zhang, B. Tan, P. Wang, X. Cui, H. Xing, AIChE J. 66 (2020) e16236.
[3] W.T. Tsai, H.P. Chen, W.Y. Hsien, J. Loss Prev. Process Ind. 15 (2002) 65–75.
[4] J.R. Clark, J. Chem. Educ. 83 (2006) 857.
[5] M.B. Chang, J.S. Chang, Ind. Eng. Chem. Res. 45 (2006) 4101–4109.
[6] X. Zhang, Y.L. Zhao, X.Y. Li, et al., J. Am. Chem. Soc. 146 (2024) 19303–19309.
[7] H.Y. Ruan, X.Q. Wu, C.L. Liao, et al., Angew. Chem. Int. Ed. 64 (2025) e202419302.
[8] J. He, H. Meng, X. Wang, Y. Xu, L. Feng, Sens. Actuator. B: Chem. 418 (2024) 136335.
[9] J. Zhu, J. Hu, H. Xiao, et al., Sep. Purif. Technol. 331 (2024) 125614.
[10] G. Xu, T. Ke, R. Fan, et al., Adv. Sci. 12 (2025) 2411083.
[11] Y. Zhu, Y. Zhou, Z. Ji, W. Zhang, M. Wu, Sep. Purif. Technol. 353 (2025) 128373.
[12] Y.L. Zhao, X. Zhang, M.Z. Li, J.R. Li, Chem. Soc. Rev. 53 (2024) 2056–2098.
[13] H. Wang, W.P. Lustig, J. Li, Chem. Soc. Rev. 47 (2018) 4729–4756.
[14] D.K.J.A. Wanigarathna, J. Gao, B. Liu, Mater. Adv. 1 (2020) 310–320.
[15] W. Xia, Z. Zhou, L. Sheng, et al., Sci. Bull. 70 (2024) 232–240.
[16] M. Wu, Z. Ji, Y. Zhou, et al., Angew. Chem. Int. Ed. 63 (2024) e202319674.
[17] Z. Ji, Q. Li, Y. Zhou, et al., Angew. Chem. Int. Ed. 63 (2024) e202411175.
[18] Z. Ji, Y. Zhou, Y. Zhu, et al., ACS Mater. Lett. 7 (2025) 837–844.
[19] Y. Zhou, C. Chen, R. Krishna, et al., Angew. Chem. Int. Ed. 62 (2023) e202305041.
[20] Z. Di, C. Liu, J. Pang, et al., Angew. Chem. Int. Ed. 61 (2022) e202210343.
[21] X. Huang, F. Chen, H. Sun, et al., J. Am. Chem. Soc. 146 (2024) 617–626.
[22] Y. Wang, Z.J. Jiang, D.R. Wang, W. Lu, D. Li, J. Am. Chem. Soc. 146 (2024) 6955–6961.
[23] M. Liu, X.W. Gu, C. Lin, et al., J. Mater. Chem. A 13 (2024) 1034–1041.
[24] Y. He, R. Krishna, B. Chen, Energy Environ. Sci. 5 (2012) 9107–9120.
[25] M.Y. Gao, A.A. Bezrukov, B.Q. Song, et al., J. Am. Chem. Soc. 145 (2023) 11837–11845.
[26] T. Ke, Q. Wang, J. Shen, et al., Angew. Chem. Int. Ed. 59 (2020) 12725–12730.
[27] C. Chen, H. Guan, H. Li, et al., Angew. Chem. Int. Ed. 61 (2022) e202201646.
[28] F. Xie, L. Chen, E.M.C. Morales, et al., Nat. Commun. 15 (2024) 2240.
[29] R.C. Zhao, L.H. Xie, X.M. Liu, et al., J. Am. Chem. Soc. 147 (2024) 2467–2475.
[30] Y. Han, Y. Chen, Y. Ma, et al., Chem 9 (2023) 3532–3543.
[31] W. Xia, Y. Yang, L. Sheng, et al., Sci. Adv. 10 (2024) eadj6473.
[32] A.R. Ravishankara, S. Solomon, A.A. Turnipseed, R.F. Warren, Science 259 (1993) 194–199.
[33] S. Wang, L. Zhou, H. Qin, et al., Molecules 29 (2024) 1721.
[34] R.K. Motkuri, H.V.R. Annapureddy, M. Vijaykumar, et al., Nat. Commun. 5 (2014) 4368.
[35] T.-H. Chen, I. Popov, W. Kaveevivitchai, et al., Angew. Chem. Int. Ed. 54 (2015) 13902–13906.
[36] J.W. Huang, J.J. Peng, X. Wei, et al., AICHE J. 69 (2023) e18027.
[37] J. Zheng, D. Barpaga, O.Y. Gutierrez, et al., ACS Appl. Energ. Mater. 1 (2018) 5853–5858.
[38] Y. Wang, F. Zhang, Y. Yang, et al., J. Colloid Interface Sci. 687 (2025) 439–448.
[39] W. Gong, Y. Geng, P. Gao, et al., J. Am. Chem. Soc. 146 (2024) 21806–21814.
[40] M. Sadakiyo, T. Yamada, H. Kitagawa, J. Am. Chem. Soc. 133 (2011) 11050–11053.
[41] H. Wang, Y. Zhao, F. Zhang, et al., Sci. Adv. 7 (2021) eabg0396.
[42] X.H. Xiong, L. Song, W. Wang, et al., Adv. Sci. 11 (2024) 2308123.
[43] R.T. Jerozal, J. Kim, C. Ma, et al., J. Am. Chem. Soc. 147 (2025) 7127–7136.
[44] J. Zheng, D. Barpaga, B.A. Trump, et al., J. Am. Chem. Soc. 142 (2020) 3002–3012.
[45] M. Zheng, W. Xue, T. Yan, et al., Angew. Chem. Int. Ed. 63 (2024) e202401770.
[46] H. Li, C. Liu, C. Chen, et al., Angew. Chem. Int. Ed. 60 (2021) 7547–7552.
[47] Z. Di, C. Liu, J. Pang, C. Chen, et al., Angew. Chem. Int. Ed. 60 (2021) 10828–10832.
[48] Y. Zhang, Y. Han, B. Luan, et al., J. Am. Chem. Soc. 146 (2024) 17220–17229.
[49] Y. Jiang, L. Wang, J. Hu, et al., Adv. Mater. 36 (2024) 2311140.
[50] X.J. Xie, H. Zeng, Y.L. Huang, et al., Chem 11 (2025) 102339.
[51] X.H. Xiong, Z.W. Wei, W. Wang, L.L. Meng, C.Y. Su, J. Am. Chem. Soc. 145 (2023) 14354–14364.
[52] J. Cui, Z. Zhang, L. Yang, et al., Science 383 (2024) 179–183.
[53] Y.J. Tian, C. Deng, L. Zhao, et al., Nat. Chem. 17 (2025) 141–147.
[54] L. Hou, W.X. Zhang, J.P. Zhang, et al., Chem. Commun. 46 (2010) 6311–6313.
[55] A.L. Spek, J. Appl. Crystallogr. 36 (2003) 7–13.
[56] W. Fan, X. Wang, X. Zhang, et al., ACS Central Sci. 5 (2019) 1261–1268.
[57] Y. Zhou, C. Chen, Z. Ji, et al., ACS Mater. Lett. 6 (2024) 1388–1395.
[58] Z.Y. Ji, Y. Fan, M. Wu, M. Hong, Chem. Commun. 57 (2021) 3785–3788.
[59] T. Steiner, W. Saenger, J. Am. Chem. Soc. 114 (1992) 10146–10154.
[60] M.S. Thompson, T.J. Meyer, J. Am. Chem. Soc. 104 (1982) 5070–5076.
[61] D.Z. Veljkovic, G.V. Janjic, S.D. Zaric, CrystEngComm 13 (2011) 5005–5010.
[62] G.R. Desiraju, Chem. Commun. (2005) 2995–3001.
[63] N.A. Porter, B. Giese, D.P. Curran, Acc. Chem. Res. 24 (1991) 296–304.
[64] W.T. Tsai, H.P. Chen, W.Y. Hsien, J. Loss Prev. Process Ind. 15 (2002) 65–75.
[65] Z. Zhang, S. Zhang, X. Liu, et al., J. Am. Chem. Soc. 146 (2024) 31213–31220.
[66] T.H. Chen, I. Popov, W. Kaveevivitchai, et al., Nat. Commun. 5 (2014) 5131.
[67] W. Zhang, Y. Li, Y. Wu, et al., Sep. Purif. Technol. 287 (2022) 120561.